

Available online at [www.sciencedirect.com](http://www.sciencedirect.com)**ScienceDirect**

Procedia Materials Science 9 (2015) 341 – 349

**Procedia**  
Materials Science[www.elsevier.com/locate/procedia](http://www.elsevier.com/locate/procedia)International Congress of Science and Technology of Metallurgy and Materials, SAM –  
CONAMET 2014

## Evaluation of corrosion resistance of aluminum-based alloys in bioethanol produced in Misiones

Gustavo Raúl Kramer<sup>a,\*</sup>, Claudia Marcela Mendez<sup>a</sup>, Alicia Esther Ares<sup>a</sup><sup>a</sup>*Facultad de Ciencias Exactas, Químicas y Naturales, UNaM, Félix de Azara 1552, Posadas (3300), Argentina*

---

### Abstract

Nowadays, biofuels represent a large part of renewable energies destined to substitute fossil fuels, and to reduce the negative impact on the environment. Bioethanol is obtained by alcoholic fermentation, and is used pure or mixed with other petroleum derivatives as fuel. Use, manipulation, storage and transport of these substances, at any scale, demand the implementation of materials, such as aluminum, that has excellent mechanical properties, as well as low density. Generally, these characteristics are improved by alloying aluminum with silicon (in order to decrease the thermal expansion coefficient and increase wear resistance) and magnesium (to increase hardness of the material). Potentiodynamic polarization and electrochemical spectroscopy impedance techniques were used on this research, in order to determine the corrosion resistance of Al-10wt.%Si, Al-12wt.%Si, Al-2%Mg and Al-4wt.%Mg alloys in an alcoholic electrolyte (bioethanol of Misiones province, Argentina industry). Comparing to pure aluminum, aluminum-silicon alloys presented better corrosion resistance. On the other hand, aluminum-magnesium alloys didn't have such improvement. By using optical metallographic microscope, no differences were found on the surfaces of alloys after being exposed to the alcoholic electrolyte.

© 2015 Published by Elsevier Ltd. This is an open access article under the CC BY-NC-ND license (<http://creativecommons.org/licenses/by-nc-nd/4.0/>).

Peer-review under responsibility of the Scientific Committee of SAM–CONAMET 2014

*Keywords:* Biofuels; aluminum alloys; corrosion

---

### 1. Introduction

Biofuels represent a possible solution to pollution by fossil fuels, and also respond to the need of sustainable energy.

---

\* Corresponding author. Tel.: +54 376 154664914.  
E-mail address: [grkramer@fceqyn.unam.edu.ar](mailto:grkramer@fceqyn.unam.edu.ar)

One of the most important biofuels is bioethanol, whose production and use are at constant growing nowadays [Farrelet al. (2006), Sorda et al. (2010)].

According to different studies, bioethanol is not compatible with aluminum [Sholz et al. (2006), Park et al. (2011)], but corrosion at low temperatures was not properly considered [Song et al. (2003)].

In most bioethanol related industries, regarding production or handling, aluminum-based alloys are used as structural material due to their fine mechanical properties. Usually there are aluminum-based alloys that contain silicon; these alloys stand out because of their wear resistance. Aluminum-based alloys that contain magnesium present good hardness and resistance [Totten and MacKenzie (2003)].

The aim of this paper is to study the corrosion behavior of commercial aluminum and aluminum-based alloys, when they are exposed to a corrosion environment composed by alcohol, which comes from sugar cane fermentation (produced in Misiones, Argentina). Also, electrochemical impedance spectroscopy (EIS) technique is used in order to understand even better the corrosion process of aluminum an aluminum-based alloys.

## 2. Materials and methods

### 2.1. Materials

Commercial aluminum (99.9%) and aluminum-based alloys with silicon (Al-10wt.%Si and Al-12wt.%Si) and magnesium (Al-2wt.%Mg y Al-4wt.%Mg) were used as test materials.

The surfaces of these materials were polished using SiC papers (#600 - #1500) before every assay.

Bioethanol (92°-96°, pH = 6) produced in “Ingenio Azucarero San Javier”, Misiones, Argentina, was used as electrolyte.

### 2.2. Methods

Corrosion resistance of all samples was analyzed using potentiodynamic polarization methods. These assays were carried out in a Gamry Reference 600 potentiostat, with a scan speed of 0.16 mV/s, from -0.4 V to 0.4 V (vs. open circuit potential, OCP), using an electrochemical cell with three conventional electrodes and a Ag/AgCl/KCl(sat) reference electrode, at 25 °C of temperature. Polarization resistance method was applied on the results.

Interaction between the metal surface and the electrolyte (bioethanol) were studied with electrochemical impedance spectroscopy (EIS) techniques. Previous to the assays, all samples were submerged in the electrolyte during 16 hours and OCP was read during that time. After immersion, EIS technique was applied, using a Gamry Reference 600 potentiostat, with a sinusoidal voltage of  $\pm 10$  mV, between 100 kHz and 0.001 Hz of frequency, at 25 °C of temperature.

Due to low conductivity of the ethanol, a 3% solution of  $\text{SO}_4\text{Na}_2$  was used as electrolyte for EIS techniques, because of its good conductivity and low corrosivity on aluminum [Park et al. (2011)].

Exposed surfaces of all samples were observed before and after every test using a NIKON Epiphot TME metallographic microscope with 100x of magnification.

## 3. Results and discussion

### 3.1. Potentiodynamic polarization

In Fig. 1, potentiodynamic polarization curves of Al-Si alloys and commercial aluminum are compared.

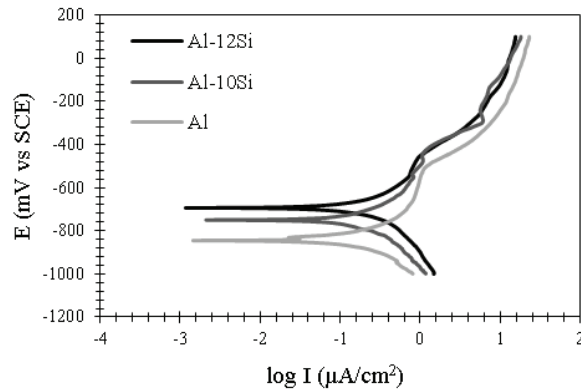


Fig. 1. Polarization curves of pure Al and Al-Si alloys.

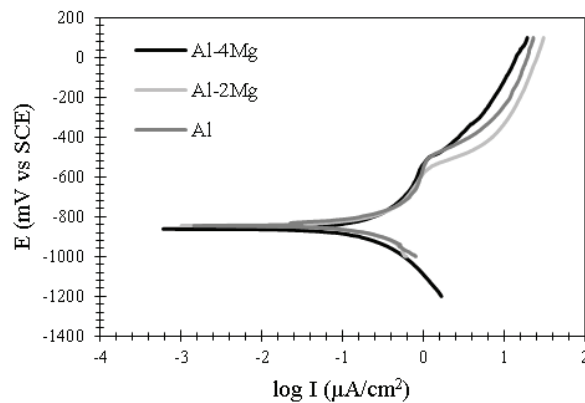


Fig. 2. Polarization curves of pure Al and Al-Mg alloys.

In Fig. 2, potentiodynamic polarization results of Al-Mg alloys and pure aluminum also are compared. Table 1 shows the results of corrosion rates.

Table 1. Parameters obtained by polarization resistant method ( $R_p$ ).

Material	$R_p$ (mV/ $\mu$ A/cm <sup>2</sup> )	$i_{corr}$ ( $\mu$ A/cm <sup>2</sup> )
Al-12wt.%Si	209.180	0.094
Al-10wt.%Si	202.177	0.113
Al	204.995	0.106
Al-2wt.%Mg	207.531	0.105
Al-4wt.%Mg	245.647	0.088

From polarization curves and Table 1 data it can be deduced that there is a similar behavior for all materials when they are analyzed without previous immersion in the electrolyte. The differences found on corrosion potentials are due to the alloyed metal effect on the base material. In Al-Si alloys, corrosion potential increased with the increase of Si content in the alloy; in Al-Mg alloys, corrosion potential was not modified with the Mg content.

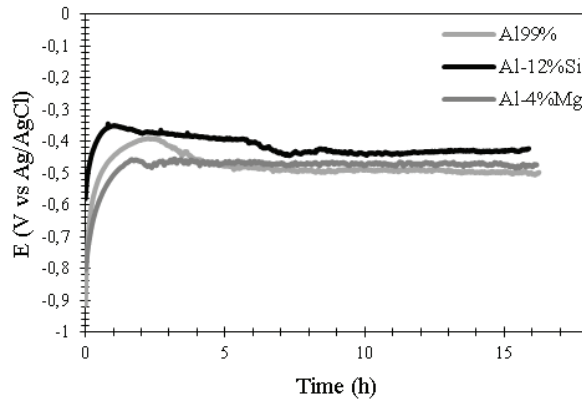


Fig. 3. Evolution of open circuit potential (EOC).

### 3.2. EIS

Fig. 3 presents the results of OCP measured during 16 hours of immersion, previous to the EIS assays. For all samples, potential was raised and subsequently stabilized, probably because of the formation of a resistive layer on exposed surfaces.

EIS results of Al-Si alloys are shown in Fig. 4 (Nyquist diagram) and Fig. 5 (Bode diagram). The system was fitted to an equivalent electric circuit presented in Fig. 6, which proves the formation of a porous oxide layer on the alloy when it is exposed to the corrosive medium.

Electric analogies of the components are:  $R_s$ : ohmic resistance of the electrolyte,  $CPE_2$ : constant phase element, similar to a capacitance of the oxide layer,  $R_2$ : oxide layer resistance,  $CPE_1$ : constant phase element due to a double layer capacitance, and  $R_1$ : charge transference resistance.

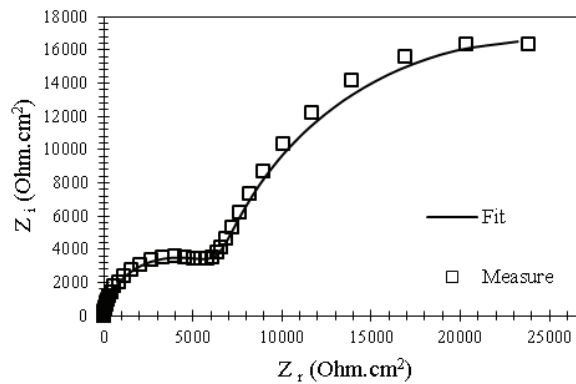


Fig. 4. Nyquist diagram for Al-12wt.%Si.

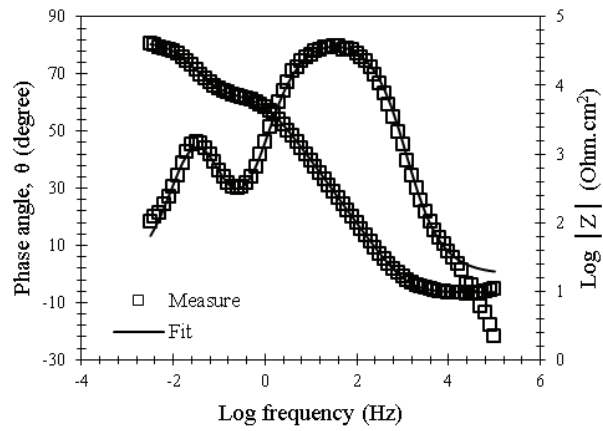


Fig. 5. Bode diagram for Al-12wt.%Si.

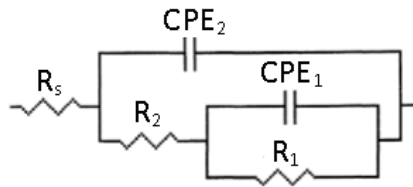


Fig. 6. Equivalent electric circuit of Al-Si/Bioethanol system.

In Figs. 7 and 8, the EIS results for Al-Mg/ethanol system are presented.

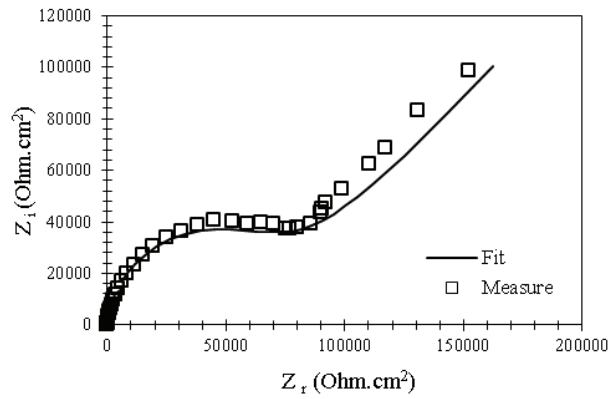


Fig. 7. Nyquist diagram for Al-4%Mg.

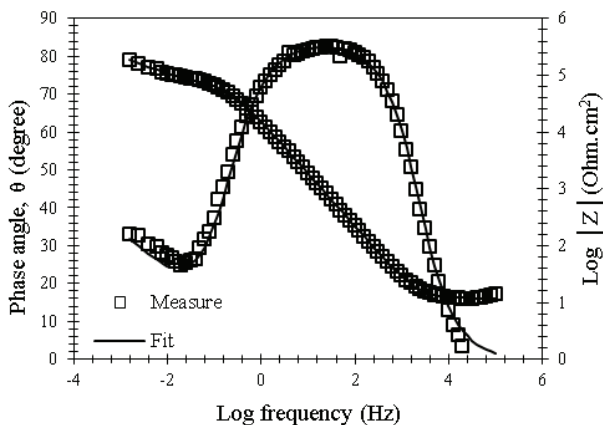


Fig. 8. Bode diagram for Al-4%Mg.

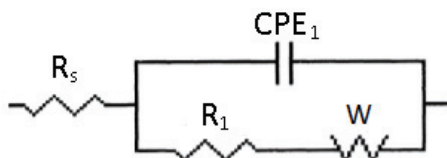


Fig. 9. Equivalent electric circuit for Al-Mg/Bioethanol system.

By applying electric circuit analogies to the process, the model of Fig.9 was fitted, where  $R_s$ : ohmic resistance of the electrolyte,  $CPE_1$ : constant phase element,  $R_1$ : resistance, and  $W$ : Warburg resistance. Results indicated that cathodic reaction is controlled by chemical species diffusion through the metal-solution interface. This phenomenon might be explained by the fact that alloying metal Mg, or precipitated intermetallic  $Al_3Mg_2$ , are more active than aluminum, and react with oxygen that diffuses towards the metal-solution interface. This is why cathodic reactions depend on oxygen diffusion [Totten and MacKenzie (2003)], and also due to a thicker layer that makes diffusion of active species through it more difficult.

Nyquist and Bode diagrams of pure or commercial aluminum (99.9%) are shown in Figs.10 and 11, respectively.

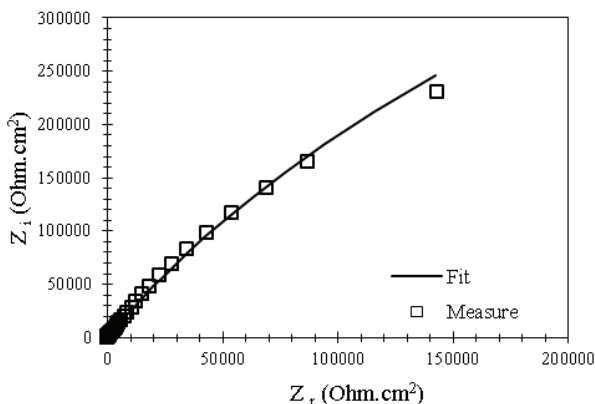


Fig. 10. Nyquist diagram for pure aluminum (99wt.%).

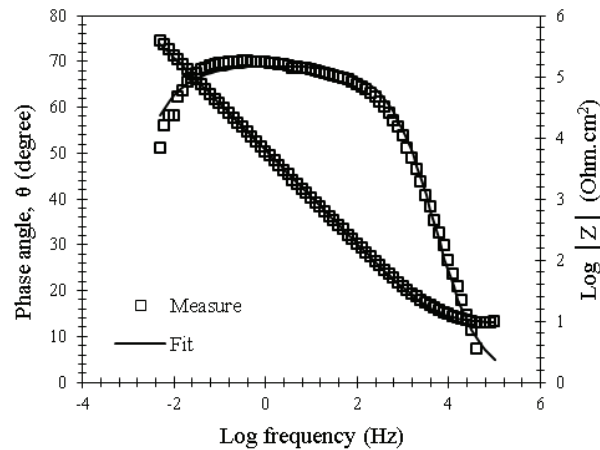


Fig. 11. Bode diagram for pure aluminum (99wt.%).

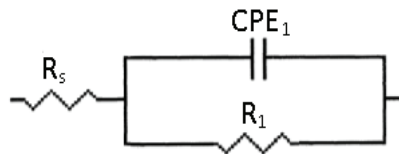


Fig. 12. Equivalent electric circuit for Al/Bioethanol system.

This behavior can be due to the presence of an oxide layer, with a constant phase element and a resistive element combination in the equivalent circuit [Huang et al. (2007)]. This is the case of pure aluminum.

Results were fitted obtaining an equivalent electric circuit, presented in Fig. 12, where  $R_s$ : ohmic resistance of the electrolyte,  $CPE_1$ : constant phase element, and  $R_1$ : resistance.

On Table 2 there can be seen electric circuit components values of all alloys.

Table 2. Parameter values of equivalent electric circuits of all alloys.

Material	Parameter							
	$R_s$ (Ohm $cm^2$ )	$R_1$ (Ohm $cm^2$ )	$CPE_1$ (F/ $cm^2$ )	n	$R_2$ (Ohm $cm^2$ )	$CPE_2$ (F/ $cm^2$ )	n	W (Ohm/s)
Al-12wt.Si	9.7	$3.49 \times 10^4$	$3.73 \times 10^{-4}$	$9.41 \times 10^{-1}$	$7.58 \times 10^3$	$2.30 \times 10^{-5}$	$9.28 \times 10^{-1}$	-
Al-10wt.Si	10.1	$6.75 \times 10^5$	$6.77 \times 10^{-5}$	$8.22 \times 10^{-1}$	$3.62 \times 10^4$	$1.45 \times 10^{-5}$	$9.11 \times 10^{-1}$	-
Al-2wt.Mg	10.9	$9.91 \times 10^4$	$6.24 \times 10^{-5}$	$9.22 \times 10^{-1}$	-	-	-	$8.1 \times 10^{-5}$
Al-4wt.Mg	11.7	$6.98 \times 10^4$	$6.21 \times 10^{-5}$	$9.32 \times 10^{-1}$	-	-	-	$1.26 \times 10^{-4}$
Al (99wt.%)	9.25	$1.67 \times 10^6$	$3.59 \times 10^{-6}$	$7.69 \times 10^{-1}$	-	-	-	-

### 3.3. Metallographic optical microscopy

Fig. 13 contains images obtained by metallographic optical microscopy of samples surfaces. There is no difference between alloys surfaces before and after polarization assays. Absence of pitting was observed, without corrosion products.

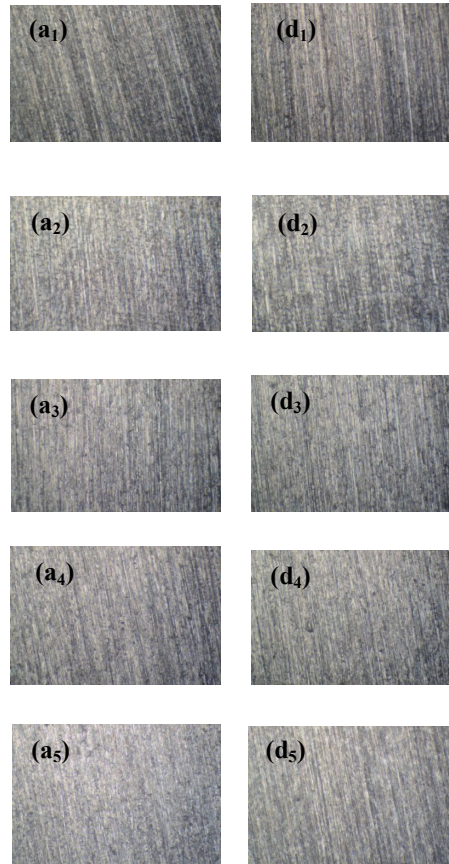


Fig. 13. Comparison of alloys surfaces before (a1: Al-10wt.%Si, a2: Al-12wt.%Si, a3: Al-2wt.%Mg, a4: Al-4wt.%Mg, a5: 99wt.%Al) and after (d1: Al-10wt.%Si, d2: Al-12wt.%Si, d3: Al-2wt.%Mg, d4: Al-4wt.%Mg, d5: 99wt.%Al) exposure to corrosive medium (magnification of 100x).

#### 4. Conclusion

The main conclusions of the present research are:

- Presence of alloying elements, such as silicon, modifies the corrosion potential when analyzed without previous immersion.
- Long exposure of materials to bioethanol allows the formation of a resistive layer, evidenced by the raise of OCP.
- EIS results let to identify the resistive layer formed on the alloys as porous, semipermeable and protective.
- For Al-Mg alloys, cathodic reactions were controlled by diffusion of oxidant species through the active surface.
- Among studied materials in this research, Al-10wt.%Si and 99wt.%Al have better behavior due to their high resistance values on the EIS and polarization tests.
- EIS and potentiodynamic polarization techniques were appropriate to study the alloy/bioethanol systems.
- Future works tend to study in detail the formation of resistive layers on samples throughout time.



## Acknowledgements

Authors wish to thank: the Ingenio Azucarero San Javier for its collaboration with donations of regional bioethanol samples, the FONCyT-ANPCyT (PICT-2012-2952) for funding the present investigation, and the CONICET for G. R. Kramer's grant.

## References

- Farrel, A., Flevin, R. J., Turner, B., 2006. Ethanol can contribute to energy and environmental goals. *Science* 311, 506-508.
- Huang, Y., Esra, K., Mansfeld, F., 2007. Evaluation of the corrosion resistance of anodizing aluminum samples using electrochemical impedance spectroscopy, Annual Graduate student research symposium. Los Angeles, California, United State.
- Park, I., Yoo, Y., Kim, J., 2011. Corrosion characteristics of aluminum alloys in bio-ethanol blended gasoline fuel: Part 1. The corrosion properties of aluminum alloy in high temperature fuels. *Fuel* 90, 1208-1214.
- Park, I., Yoo, Y., Kim, J., 2011. Corrosion characteristics of aluminum alloys in bio-ethanol blended gasoline fuel: Part 2. The effect of dissolved oxygen in the fuel. *Fuel* 90, 633-639.
- Sholz, M., Ellerneir, J., 2006. Corrosion behavior of different aluminium alloys in fuel containing ethanol under increased temperatures. *Metaralwissenschaft und Werkstofftechnik* 37, 842-851.
- Song, G. L., Liu, M., 2013. Corrosion and electrochemical evaluation of an Al-Si-Cu aluminum alloy in ethanol solution. *Corrosion Science* 72, 73-81.
- Sorda, G., Banse, M., 2010. An overview of biofuel policies across the world. *Energy Policy* 38, 6977-6988.
- Totten, G., MacKenzie, S., 2003. *Handbook of Aluminum: Vol 1: Physical Metallurgy and Processes*, Marcel Dekker, Inc.